Evolution of crystal structure with the oxygen content in the LaMn$_{0.9}$Cr$_{0.1}$O$_{3+\delta}$ $(3.00 \leqslant 3 + \delta \leqslant 3.12)$ compound

L. Morales[a] and A. Caneiro[b,*]

[a] CONICET, Centro Atómico Bariloche-Instituto Balseiro, Av. E. Bustillo 9500, S. C. de Bariloche, Rio Negro (8400), Argentina
[b] CNEA-Centro Atómico Bariloche-Instituto Balseiro, Unidad de Actividad Technologia de Materiales y Dispositivos, Av. E. Bustillo 9500, S. C. de Bariloche, Rio Negro (8400), Argentina

Abstract

We report the structural evolution as a function of oxygen content for LaMn$_{0.9}$Cr$_{0.1}$O$_{3+\delta}$($3.00 \leqslant 3 + \delta \leqslant 3.12$) in samples prepared with accurate control of the oxygen content. The relationship between the structural parameters and magnetic behavior is established using δ as control parameter. As the δ value increases, three different orthorhombic regions are found: for $\delta < \delta_c$ the distorted O′ phase $(b/\sqrt{2} < c < a)$, and for $\delta > 0.06$ two low distorted orthorhombic regions (O″ with $b/\sqrt{2} < a < c$ and O″′ with $a < b/\sqrt{2} < c$). The structural study shows a critical $\phi_c \approx 11°$ tilt angle corresponding to $\delta_c \approx 3.06$ and is related to a jump in the critical temperature and magnetic moment (μ). This ϕ_c separates FM from non-FM samples. The results are compared with those for LaMnO$_{3+\delta}$. The variation of μ as a function of oxygen content and therefore with the amounts of Mn^{4+} allowed us to discuss the role of the Cr^{3+} ion on the magnetic behavior of LaMn$_{0.9}$Cr$_{0.1}$O$_{3+\delta}$.
© 2002 Elsevier Science (USA). All rights reserved.

Keywords: Cr-doped LaMnO$_{3+\delta}$; Perovskite structure; Oxygen stoichiometry

1. Introduction

The ideal cubic perovskite structure, with general formula ABX_3, consists essentially of a framework of BX_6 octahedra linked by their corners, with a large 12 coordinated A cation. If the A, B, and X ions are not of the ideal relative size, there is no adjustable atom position parameter and a structural distortion occurs, which depends on the sizes and bonding character of the cations.

In ABO_3 compounds, the magnetic cation–anion–cation exchange interaction depends on the electron configuration of the B cations, on the distances between the ions, and on the subtended bond angle B–O–B. The strength of the magnetic exchange interaction between manganese ions is dependent on the magnitude of this angle.

The LaMnO$_{3+\delta}$ perovskite has been extensively studied due to the rich magnetic phase diagram and the relationship with the structural distortions induced by the variation of oxygen content [1–3]. The stoichiometric compound has O′ orthorhombic symmetry $(b/\sqrt{2} < c < a)$ with an A-type antiferromagnetic order. This order consists of ferromagnetic interactions (FM) in the (001) plane and antiferromagnetic (AFM) interactions between FM planes. This magnetic configuration is related to orbital ordering between empty and occupied e_g states in the a–b plane and AFM superexchange interactions (SE) between two manganese with three half-filled t_{2g} orbitals. LaMnO$_3$ contains trivalent manganese and due to the strong Hund's coupling, the manganese ions adopt a high spin configuration $t_{2g}^3 e_g^1$. According to the Jahn–Teller theorem, a distortion of the local octahedral environment is energetically favorable. This distortion is accomplished by lengthening two of the Mn–O bonds which lowers the energy of the occupied $3d_{z^2}$ orbitals, relative to the empty $3d_{x^2-y^2}$ orbitals. A small FM component is always present due to the antisymmetric Dzialoshinski exchange coupling $(\mathbf{D}_{ij}.\mathbf{S}_i \times \mathbf{S}_j)$ introduced by the tilt of the MnO$_6$ octahedra.

*Corresponding author. Fax: +54-2944-445299.
E-mail addresses: moralesl@cab.cnea.gov.ar (L. Morales), caneiro@cab.cnea.gov.ar (A. Caneiro).

The cooperative Jahn–Teller distortion (JTD) can be suppressed either by temperature or by increasing the oxygen content. The latter changes the average Mn valence raising the hole concentration. Thus, the increment of Mn^{4+} favors FM order due to the existence of Mn^{3+}–O–Mn^{4+} double exchange (DE) interaction and progressively removes the JTD.

The substitution of Mn by other ions has been extensively studied, because it alters the magnetic interactions in the Mn–O network modifying the magnetic phase diagram.

In the case of Cr-doped manganites, the Cr ion is incorporated as Cr^{3+} in the *B* site of the perovskite structure. Since Cr^{3+} is isoelectronic with Mn^{4+} ($3d^3$), it was suggested that this ion may play a role in the DE mechanism equivalent to that of Mn^{4+}. The effect of Mn substitution by Cr on the magnetic properties of manganites is not clear in the literature.

An early neutron diffraction study of the $LaMn_{1-x}Cr_xO_3$ solid solution indicates that the *A*-type AFM structure of $LaMnO_3$ persists only for very small concentrations of Cr^{3+}, while the *G*-type AFM of $LaCrO_3$ is found over a wide composition range. The introduction of Cr^{3+} into the *A*-type AFM structure leads to a spin reversal of some of the Mn^{3+} nearest neighbors increasing the ferromagnetic moment [4]. Later some authors suggested a ferromagnetic Cr^{3+}–O–Mn^{3+} exchange interaction (SE or DE) since Cr^{3+} is isoelectronic with Mn^{4+} [5–8].

However, it was claimed that the effective DE interaction is not established between Cr^{3+} and Mn^{3+} ions and only the superexchange one takes place [9,10]. Finally, a recent publication suggests the presence of two different DE processes in this system: a strong Mn^{3+}–O–Mn^{4+} DE interaction and a weak Mn^{3+}–O–Cr^{3+} one [11,12].

It is worth mentioning that in all the studies performed on $LaMn_{1-x}Cr_xO_3$ ($0 < x < 1$) samples, the effect of oxygen content on their crystal structure and magnetic behavior have not been analyzed. Some of the studies report only the amount of Mn^{4+} for the as-made samples which clearly indicate the presence of a wide range of oxygen non-stoichiometry.

The aim of this paper is to study in detail the effect of oxygen content on crystal structure and magnetic behavior of a low Cr-doped $LaMnO_3$ manganite, namely $LaMn_{0.9}Cr_{0.1}O_{3+\delta}$. For this purpose we have varied δ over a wide range ($0 < \delta < 0.12$) and followed the evolution of the crystal structure and magnetic response.

2. Experimental procedure

A sample with nominal composition $LaCr_{0.1}Mn_{0.9}O_{3+\delta}$ was prepared by the liquid-mix method (LMM) [13].

Stoichiometric proportions of La_2O_3, CrO_3 and metallic Mn (all reactants with purity better than 99.99%) were dissolved in a dilute solution of nitric acid and dried at 200°C. The obtained nitrate was dissolved in a solution of citric acid and 2% (v/v) of ethylene glycol. The obtained material was preheated slowly to 300°C, 500°C, 600°C and 800°C taking 24 h for each step under a controlled atmosphere (Ar + O_2) and finally treated at 1150°C for 12 h in air. Before this, the La_2O_3 and the CrO_3 were dried at 1200°C for 12 h and 220°C for 2 h, respectively, in order to remove absorbed or chemically bonded products such as CO_2 or H_2O.

X-ray powder diffraction data were collected on a Philips PW-1700 diffractometer using Cu$K\alpha$ radiation and a graphite monochromator. The data were obtained in the $20° \leqslant 2\theta \leqslant 120°$ range, with steps of $0.02°$ and counting time of 15 s per step. Structural refinements were performed using the Rietveld method (Fullprof) [14].

Equilibrium $p(O_2)$ measurements as a function of "δ" and T in $LaMn_{0.9}Cr_{0.1}O_{3+\delta}$ were performed using thermogravimetric (TG) equipment consisting of a symmetrical thermobalance based on a Cahn 1000 electrobalance coupled to an electrochemical system for measuring and controlling $p(O_2)$ [15]. Samples with controlled oxygen content ($3.00 \leqslant 3 + \delta \leqslant 3.12$) were prepared by annealing them at different temperatures T and $p(O_2)$ values during 24 h and later quenching at liquid nitrogen temperature. We have used this method to control the oxygen content before to study several complex oxides systems [3,16,17]. Although oxygen excess in the perovskite structure is not possible due to its compact character, we express the oxygen content as "$3 + \delta$" for clarity, instead of the chemical formula $La_{3/3+\delta}(Mn_{0.9}Cr_{0.1})_{3/3+\delta}O_3$ with cation's vacancies.

D.c. magnetization (M) measurements vs. temperature (T) under $H = 100$ Oe and M vs. magnetic field (H) at 5 K were performed with a commercial Quantum Design (SQUID) magnetometer.

3. Results and discussion

3.1. Oxygen non-stoichiometry

The $\log\{p(O_2)\}$ vs. $3 + \delta$ curves for $LaCr_{0.1}Mn_{0.9}O_{3+\delta}$ at 1000°C and 900°C are shown in Fig. 1. Two extra data points (800°C and 700°C) taken under pure oxygen were added to this figure. The rapid variation of $p(O_2)$ for $\log\{p(O_2)\} < -5$ for the 1000°C isotherm indicates the existence of a stoichiometric $LaMn_{0.9}Cr_{0.1}O_3$ compound. Therefore, considering that the oxygen stoichiometric compound is formed at 1000°C within the range $-7 < \log\{p(O_2)\} < -5$ it is possible to determine the

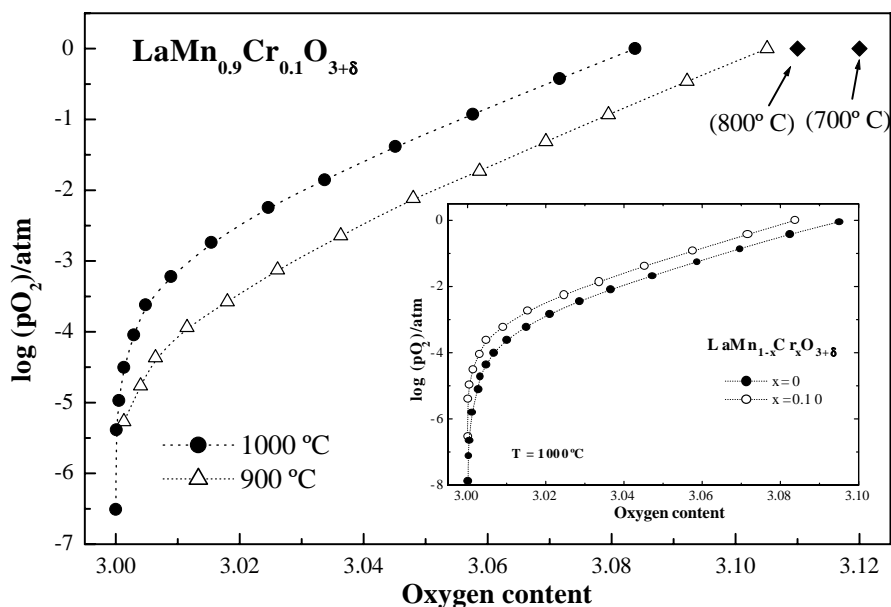Fig. 1. Isotherms of $\log\{p(O_2)\}$ vs. oxygen content $(3+\delta)$ for $LaMn_{0.9}Cr_{0.1}O_{3+\delta}$ compound at $T = 1000°C$ and $900°C$. Extra points under 1 atm. of oxygen at $T = 800°C$ and $700°C$ are included and marked in this plot.

absolute oxygen concentration of the samples as a function of $p(O_2)$ with high accuracy.

The shape of this curve reveals an important range of oxygen non-stoichiometry for this material. In the inset of this figure, the isotherm of $1000°C$ is compared with that of $LaMnO_{3+\delta}$ [3]. It can be seen that the oxygen non-stoichiometry for the Cr-doped samples is lower than that of the undoped material but is still significant. This is consistent with the fact that the end member of the $LaMn_{1-x}Cr_xO_3$ family, the pure $LaCrO_3$ phase, does not display oxygen non-stoichiometry.

Therefore, oxygen non-stoichiometry may play an important role on the structural and magnetic properties for the Cr-doped manganites as it is well known to do for $LaMnO_{3+\delta}$.

3.2. Structural study

The X-ray diffractograms of all the samples with $0 < \delta < 0.12$ show the presence of the ABO_3 perovskite phase without impurity phases. For $0 \leqslant \delta \leqslant 0.10$ the samples had orthorhombic symmetric with space group *Pnma*. For the sample with $\delta = 0.11$, the X-ray data indicated a mixture of orthorhombic (*Pnma*) and rhombohedral symmetry ($R\bar{3}c$). Finally for $\delta = 0.12$ only the rhombohedral symmetry is present. Then, around $\delta = 0.11$ the data show the existence of a narrow range of two-phase field which separates both symmetries.

In Table 1 are shown the structural parameters and the corresponding errors obtained from the Rietveld refinements.

The evolution of the cell parameters for $LaMnO_{3+\delta}$, $LaMn_{0.9}Cr_{0.1}O_{3+\delta}$, and the steric factor of the last compound (defined as $s = \overline{d(La-O)}/[\sqrt{2}\,\overline{d(B-O)}]$) as a function of the oxygen content are shown in Figs. 2(a), (b), and (c), respectively.

Two differences appear relative to $LaMnO_{3+\delta}$: on the one hand, we see that the orthorhombic distortion is lower, and on the other, the phase boundary $(O + R)/R$ is shifted to a higher oxygen content value. This may be because the ionic radius of Cr^{3+} (0.615) is larger than that of Mn^{4+} (0.58). The rhombohedral symmetry appears in the Cr-doped samples and undoped one at the same oxygen content $(\delta = 0.11)$, but for $LaMn_{0.9}Cr_{0.1}O_{3.11}$ we observe the coexistence of two phases $(R + O'')$, while for $LaMnO_{3.11}$ we have only the R symmetry.

As oxygen content increases, the orthorhombic phase evolves changing the relationship between cell parameters as is shown in Table 1 and Fig. 2(b). Three different regions are distinguishable depending on the δ value: (I) for $0 \leqslant \delta \leqslant 0.05$, $b/\sqrt{2} < c < a$ (in *Pnma* setting) and corresponds to the well-known O' phase, (II) for $\delta = 0.06$, a becomes smaller than c $(b/\sqrt{2} < a < c)$ (O''), and (III) for $0.07 \leqslant \delta \leqslant 0.10$ the parameter a is still lower and becomes the smallest $(a < b/\sqrt{2} < c)$ (O'''). The so-called O-type structure with $c \leqslant b/\sqrt{2} \leqslant a$ is not found in the present work. This is in agreement with results of other authors for the $LaMnO_{3+\delta}$ system [2,3,19]. It can be seen that the phase boundaries O'/O'' and O''/O''' of the $LaMnO3 + d$ are shifted to higher values of oxygen content than those of Cr-doped perovskite. On the other hand, a region of coexistence of two

Table 1
Structural data of LaMn$_{0.9}$Cr$_{0.1}$O$_{3+\delta}$

| $3+\delta$	SG	a (Å)	b (Å)	c (Å)	Vol (Å^3)	B–O$_1^m$ (Å)	B–O$_2^s$ (Å)	B–O$_2^l$ (Å)	ϕ (°)	ω (°)
3.00	$Pnma$	5.6648(1)	7.7366(1)	5.5392(1)	242.766(4)	1.991(9)	1.918(3)	2.114(9)	13.7(1)	10.9(2)
3.01	$Pnma$	5.6455(2)	7.7435(2)	5.5390(2)	242.140(4)	1.988(4)	1.918(6)	2.110(8)	13.2(1)	10.9(1)
3.02	$Pnma$	5.6280(1)	7.7547(1)	5.5424(2)	241.887(4)	1.985(2)	1.927(7)	2.093(7)	12.4(1)	10.8(2)
3.03	$Pnma$	5.5987(2)	7.7631(3)	5.5388(2)	240.744(4)	1.984(3)	1.932(9)	2.073(8)	11.9(1)	10.6(4)
3.04	$Pnma$	5.5698(1)	7.7714(1)	5.5348(1)	239.574(4)	1.981(2)	1.955(7)	2.035(7)	11.3(1)	10.3(2)
3.05	$Pnma$	5.5490(1)	7.7983(1)	5.5416(1)	239.801(4)	1.986(2)	1.974(8)	2.003(8)	10.9(1)	9.7(2)
3.06	$Pnma$	5.5209(1)	7.7991(1)	5.5379(1)	238.448(4)	1.983(2)	1.975(7)	1.994(8)	10.59(7)	9.8(3)
3.07	$Pnma$	5.5122(1)	7.7991(1)	5.5392(1)	238.134(4)	1.985(2)	1.976(7)	1.987(7)	10.81(6)	9.6(3)
3.08	$Pnma$	5.5039(1)	7.7931(1)	5.5383(1)	237.552(4)	1.982(2)	1.968(7)	1.983(7)	10.55(6)	8.9(3)
3.09	$Pnma$	5.4998(1)	7.8830(1)	5.5374(1)	237.189(4)	1.977(2)	1.973(9)	1.98(9)	9.97(9)	9.1(4)
3.10	$Pnma$	5.4951(1)	7.7822(1)	5.5365(1)	236.763(4)	1.975(2)	1.968(8)	1.977(8)	9.94(7)	8.6(3)
3.11	$Pnma+$	5.4928(1)	7.7765(1)	5.5368(1)	236.469(4)					
	$R\bar{3}c$	5.5351(1)	5.5351(1)	13.3410(1)	354.045(4)					
3.12	$R\bar{3}c$	5.5318(1)	5.5318(1)	13.3383(2)	353.483(3)	1.968(4)	1.968(4)	1.968(4)	8.62(6)	8.62(6)
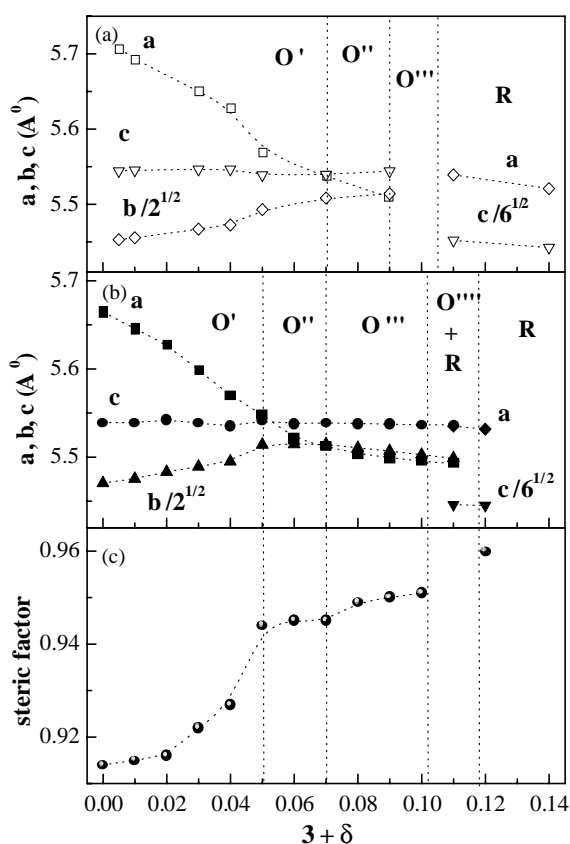
Fig. 2. Evolution of the cell parameters for LaMnO$_{3+\delta}$, LaMn$_{0.9}$Cr$_{0.1}$O$_{3+\delta}$ and the steric factor for LaMn$_{0.9}$Cr$_{0.1}$O$_{3+\delta}$ as a function of the oxygen content. The different orthorhombic regions correspond to those denoted as O', O'', and O'' '. The O'' ' + R regions is the two phase field, and R corresponds to the rhombohedral phase.

orthorhombic phases (O + O') was not detected for LaMn$_{0.9}$Cr$_{0.1}$O$_{3+\delta}$ as has been reported for the Cr-free compounds [18].

As the steric factor goes up with oxygen content (Fig. 2c), the structure becomes more symmetric. This is a consequence of the increase of Mn^{4+} concentration which is not a Jahn–Teller ion and is smaller than Mn^{3+}. So the distortion of the structure is reduced and the coordination number of the A site is increased. Following the evolution of the steric factor, it can be observed that a rapid increase of s occurs up to $3+\delta \approx 3.05$ within the O' phase region. Within the region of the O'' phase ($3.05 < 3+\delta < 3.07$) s remains practically constant and increases slightly for the O'' ' region.

The volume of the unit cell shown in Table 1 decreases as the oxygen content increases. This is consistent with the substitution of Mn^{3+} by Mn^{4+}.

In what follows we denote both ions at the B site of the structure, Mn and Cr, as B.

The B–O bond distances and the mean distortion of the BO_6 octahedron are shown in Figs. 3(a) and (b), respectively. Fig. 3(a) shows that a strong JTD is present at low oxygen content despite the presence of 10% of Cr^{3+} ions. The range of high JTD corresponds to the O' phase. As expected, the differences between the B–O distances for LaMn$_{0.9}$Cr$_{0.1}$O$_{3+\delta}$ are lower than those of LaMnO$_{3+\delta}$.

For samples in the range $0.06 \leqslant \delta \leqslant 0.10$ the octahedra became less distorted and this is associated with the O'' and O'' ' regions. Finally, for $\delta = 0.12$ (rhombohedral phase) the octahedra are regular.

The mean distortion of the octahedron, defined as $\Delta d = (1/N) \sum_{i=1}^{N} [(d_i - \langle d \rangle)/\langle d \rangle]^2$, shown in Fig. 3(b) summarizes the evolution discussed above. One point to emphasize here is the sensitivity of the structure to small changes in the oxygen content mainly at the O' phase. All these results underscore the importance of knowing precisely the oxygen content of the samples for a correct characterization of the physical properties.
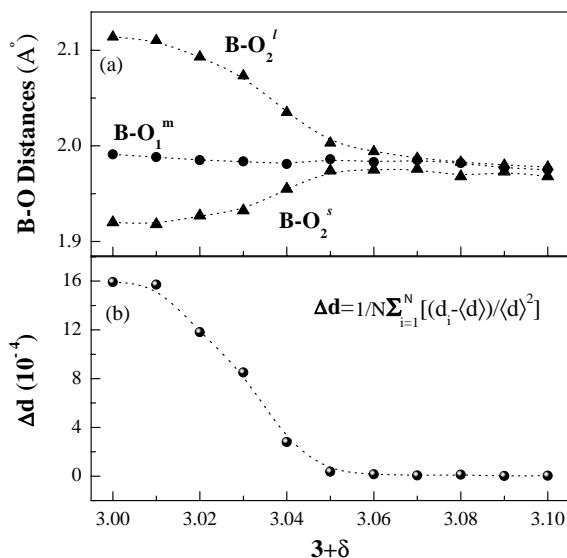
Fig. 3. Evolution of the *B*–O distances, and the mean distortion of the BO_6 octahedra vs. the oxygen content.

Fig. 4. Evolution of the critical temperature (T_N, T_C) and the magnetic moment μ as a function of the oxygen content, respectively. The μ values at 5 K and 50 KOe of the $LaMn_{0.9}Cr_{0.1}O_{3+\delta}$ samples are compared with those of $LaMnO_{3+\delta}$.

The other parameters that are associated with octahedral distortion are the tilt angle ϕ ($\phi = [180 - (B - O_1 - B)]/2$) and the rotation angle ω ($\omega = [180 - (B - O_2 - B)]/2$). Both angles decrease as oxygen content increases and reflect the loss of structural distortion as the Mn^{4+} content increases (see Table 1). The difference between these angles diminishes when the perovskite becomes more regular and both angles take the same value for the rhombohedral symmetry. For the less distorted orthorhombic phases ($\delta > 0.05$) and for the rhombohedric one ϕ and ω remain below $11°$. This value plays a significant role on the magnetic behavior as will be discussed later.

3.3. Magnetic correlation

The magnetic transition temperature (T_N, T_C) and the magnetic moment (μ) at 5 K vs. the oxygen content $(3 + \delta)$ are shown in Figs. 4(a) and (b), respectively. The values in Fig. 4(a) were determined by differentiation of the magnetization curves (M) vs. temperature (T) at $H = 100$ Oe and those of Fig. 4(b) from the M vs. H measurements at $T = 5$ K and $H = 50$ kOe. The critical temperature shows a minimum for $3 + \delta \approx 3.02$ and increases fast in the region $3.02 \leqslant 3 + \delta \leqslant 3.05$. The magnetic moment μ increases rapidly with oxygen content up to the boundary between the O' and O'' regions $(3 + \delta \approx 3.05)$. Both the critical temperature and μ remain practically constant for $3 + \delta \geqslant 3.06$. For the $LaMnO_{3+\delta}$ system, T_C and μ fall for high δ values $(3 + \delta > 3.11)$ but this behavior is not found for the Cr-doped samples at least for the oxygen content values measured in the present work. Larger δ values are needed in order to confirm this. Another difference relative to the
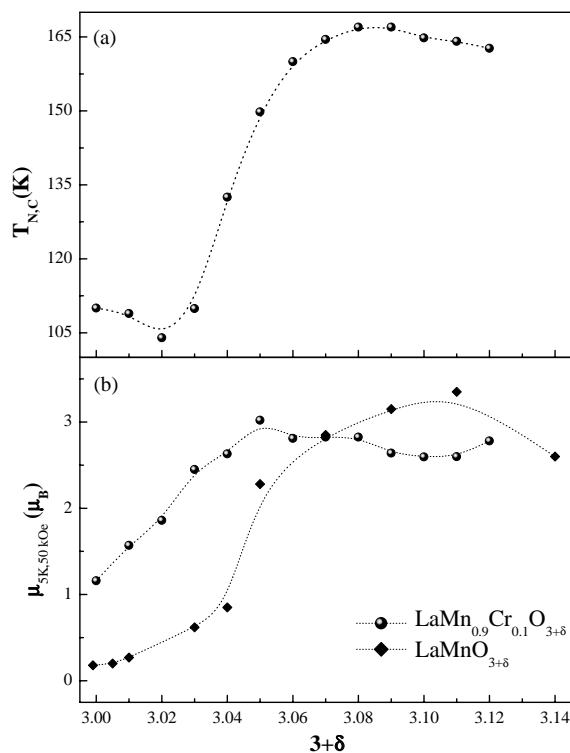
$LaMnO_{3+\delta}$ compound appears for the μ value at the O' phase. The reported values of μ at low oxygen contents [3] are lower than those for the $LaMn_{0.9}Cr_{0.1}O_{3+\delta}$ system. This fact suggests that the Cr^{3+}–O–Mn^{3+} interaction would be an FM one. This observation is in agreement with that of Bents et al. [4] where the introduction of Cr^{3+} into the *A*-type AFM structure leads to an FM alignment of nearest neighbors increasing the ferromagnetic moment. However, at δ values higher than 0.07, μ remains lower than that of $LaMnO_{3+\delta}$. For the $LaMnO_{3+\delta}$ compound, as the oxygen content increases (and therefore that of Mn^{4+}), the FM Mn^{3+}–O–Mn^{4+} DE interaction dominates over the SE Mn^{3+}–O–Mn^{3+} one. For high values of oxygen content ($\delta > 0.11$) the AF Mn^{4+}–O–Mn^{4+} decreases the magnetization. In our case, as the oxygen content increases the AFM Cr^{3+}–O–Mn^{4+} SE interaction should be considered. The contribution of this interaction is to decrease the magnetization relative to that of $LaMnO_{3+\delta}$ as it is observed for $\delta > 0.07$.

The variation of the transition temperature and μ as a function of the tilt angle ϕ are shown in Figs. 5(a) and (b), respectively. In Fig. 5(a) a jump in $T_{N,C}$ vs. ϕ can be seen for a critical angle, ϕ_c, around $11°$. Similar behavior occurs when μ vs. ϕ is plotted (Fig. 5b)). It can be seen that both μ and the critical temperature are more sensitive to variation in ϕ than to changes in the
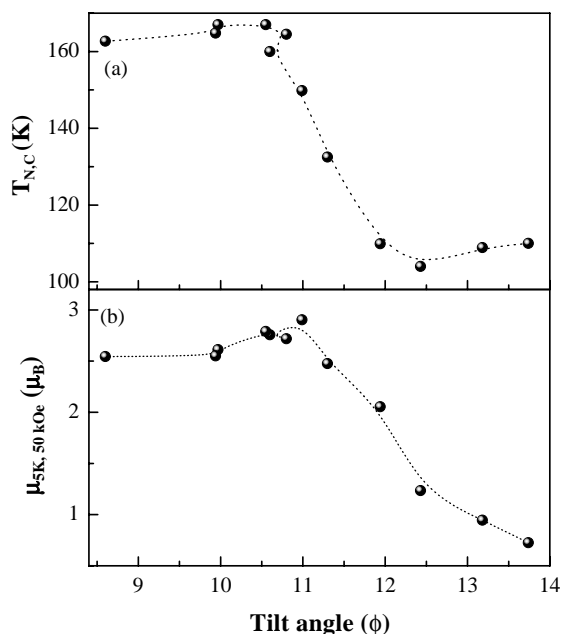
Fig. 5. Variation of the critical temperature and magnetic moment as a function of the tilt angle ϕ, respectively. A jump at $\phi = 11°$ is observed.

oxygen content. The B–O_1–B bond angle in samples with $\delta > 0.06$ is lower than ϕ_c (Table 1).

As was reported earlier by Huang et al. [2] for the LaMnO$_{3+\delta}$ system, $\phi \sim 9°$–$10°$ corresponds to an orthorhombic FM structure and $\phi \sim 12°$–$13°$ to an orthorhombic AFM one. They also report the presence of three orthorhombic phases with the same relationships between cell parameters found by us [2]. Their characterization with neutron diffraction shows that the O′ phase is associated with an AFM phase, while the other two orthorhombic phases (O″ and O″′) and the rhombohedral one with an FM structure.

Using these results and making an analogy between the Cr-doped system and the undoped one, the samples studied in the present paper can be classified as FM and non-FM ones. The critical angle $\phi_c \approx 11°$ corresponds approximately to an oxygen content value of 3.06 which is the boundary between the O′ and the O″ phases. Therefore, $3 + \delta = 3.06$ can be defined as δ_c. So, for $\delta \geqslant \delta_c$ the samples would be FM while those with more distorted octahedra ($\delta < \delta_c$) would correspond to an AFM phase or a cluster glass state caused by a competition between FM and AFM interactions.

This study allowed us to analyze the effect of Cr on the crystal structure and magnetic behavior of Cr-doped LaMnO$_3$ manganite changing progressively the Mn^{4+} concentration. Thus, as the oxygen content increases, the effect of Cr^{3+} not only depends on the Cr^{3+}–O–Mn^{3+} interaction but also on the Cr^{3+}–O–Mn^{4+} one.

Most of the studies on the effect of Cr on the magnetic behavior of manganites were made either on

samples with nominal LaMn$_{1-x}$Cr$_x$O$_3$ or compounds with a fixed amount of Mn^{4+} ($0.3 \leqslant x \leqslant 0.50$). The lack of agreement concerning the nature of the Cr^{3+}–O–Mn^{3+} interaction may be due to the presence of different competing interactions. The oxygen non-stoichiometry is crucial in order to analyze the magnetic data. Thus, the reported rhombohedral symmetry in LaMn$_{1-x}$Cr$_x$O$_3$ samples [12,20] ($x < 0.4$) may be due to oxygen excess in the samples. The rhombohedral symmetry is present in LaMnO$_{3+\delta}$ and LaMn$_{0.9}$Cr$_{0.1}$O$_{3+\delta}$ for $\delta > 0.10$. This symmetry is associated with high amounts of Mn^{4+} and therefore with the FM Mn^{3+}–O–Mn^{4+} DE interaction. The disagreement on the nature of the FM Mn^{3+}–O–Cr^{3+} interaction (SE or DE) may be due to the unnoticed presence of Mn^{4+} not only in the rhombohedral phase but also in the orthorhombic one. Moreover, the AFM Cr^{3+}–O–Mn^{4+} and Cr^{3+}–O–Cr^{3+} interactions became relevant and their contributions decrease the magnetization.

4. Conclusion

In the present paper the complete structural study of the LaMn$_{0.9}$Cr$_{0.1}$O$_{3+\delta}$ system with $3.00 \leqslant 3 + \delta \leqslant 3.12$ is reported.

The substitution of Mn^{3+} by Cr^{3+} lowers the structural distortion mainly due to the non-Jahn–Teller character of the Cr^{3+} ion and the difference in the ionic radii ($r_{Mn^{3+}} > r_{Cr^{3+}}$). The analogy with results reported in the Cr-free system allow us to correlate the magnetic behavior with the structural study. A critical structural parameter $\phi_c \approx 11°$ separates FM from non-FM samples.

The evolution of structural properties as a function of oxygen content also reveals that a small change in δ can produce a great effect on the magnetic properties especially for δ near δ_c.

Comparing the magnetic moment between undoped and Cr-doped samples with equal amounts of Mn^{4+} allowed us to analyze the magnetic contribution of the Cr^{3+}.

An extensive study of the magnetic behavior of these samples is in progress.

Acknowledgments

References

[1] A. Wold, R.J. Arnott, J. Phys. Chem. Solids 9 (1959) 176.
[2] Q. Huang, A. Santoro, J.W. Lynn, R.W. Erwin, J.A. Borchers, J.L. Peng, R.L. Greene, Phys. Rev. B 55 (1997) 14987–14999.
[3] F. Prado, R.D. Sánchez, A. Caneiro, M.T. Causa, M. Tovar, J. Solid State Chem. 146 (1999) 418–427 doi:10.1006/jssc.1999.8386.
[4] U.H. Bents, Phys. Rev. 106 (1957) 225–230.
[5] R. Gundakaram, A. Arulraj, P.V. Vanitha, C.N.R. Rao, N. Gayathri, A.K. Raychaudhuri, A.K. Cheetham, J. Solid State Chem. 127 (1996) 354–358.
[6] A. Barnabé, A. Maignan, M. Hervieu, F. Damay, C. Martin, Raveau, Appl. Phys. Lett. 71 (1997) 3907–3909.
[7] C. Osthöver, P. Grünberg, R.R. Arons, J. Magn. Magn. Mater. 177–181 (1998) 854–855.
[8] A. Maignan, C. Martin, F. Damay, M. Hervieu, B. Raveau, J. Magn. Magn. Mater. 188 (1998) 185–194.
[9] O. Cabeza, M. Long, C. Sevarac, M.A. Bari, C.M. Muirhead, M.G. Francesconi, C. Greaves, J. Phys.: Condens. Matter 11 (1999) 2569–2578.
[10] F. Rivadulla, M. Am. López-Quintela, L.E. Hueso, P. Sande, F. Rivas, R.D. Sánchez, Phys. Rev. B 62 (2000) 5678–5684.
[11] N. Kallel, J. Dhahri, S. Zemni, E. Dhahri, M.U. Oumezzine, M. Ghedira, H. Vincent, Phys. Stat. Sol. (A) 184 (2) (2001) 319–325.
[12] Y. Sun, W. Tong, X. Xu, Y. Zhang, Phys. Rev. B 63 (1–5) (2001) 174438.
[13] A. Serquis, F. Prado, A. Caneiro, Physica C 253 (1995) 339–350.
[14] Rodríguez-Carabajal, Fullprof: A Program for Rietveld Refinement and Profile Matching Análisis of Complex Powder Diffraction Patterns, Laboratoire Léon Brillouin (CEA-CNRS).
[15] A. Caneiro, P. Bavdaz, J. Fouletier, J.P. Abriata, Rev. Sci. Instrum. 53 (1982) 1072–1076.
[16] A. Serquis, A. Caneiro, F. Prado, Physica C 313 (1999) 271–280.
[17] A. Serquis, A. Caneiro, A. Basset, S. Short, J.P. Hodges, J. Jorgensen, Phys. Rev. B 63 (2001) 014508.
[18] A.K. Bogush, V.I. Pavlov, L.V. Balyko, Cryst. Res. Technol. 18 (1983) 589.
[19] C. Ritter, M.R. Ibarra, J.M. De Teresa, P.A. Algarabel, C. Marquina, J. Blasco, J. García, S. Oseroff, S.W. Cheong, Phys. Rev. B 56 (1997) 8902–8911.
[20] H. Taguchi, S. Matsu-ura, M. Nagao, H. Kido, Physica B 270 (1999) 325–331.